

# Review: Solid-state physics of halide perovskites

Jarvist Moore Frost<sup>b</sup>

<sup>a</sup>*Department of Physics, King's College London, Strand, London WC2R 2LS, UK*

<sup>b</sup>*Department of Physics, Imperial College London, Exhibition Road, London SW7 2AZ, UK*

## Abstract

Halide perovskite solar cells presented a unique opportunity to apply modern computational materials science techniques to an (initially) poorly understood new material. In this review, we recount the key understanding developed during the last five years, through a narrative review of research progress. The central enigma of the material is how it can be so defective, and yet work so well as a photovoltaic. The physical properties of the material were understood through molecular and lattice dynamic calculations, revealing the material to show large dynamic responses on a wide range of time scales. Longer length scales in the material was simulated with effective classical potentials, showing that complex domains can be generated by the interacting molecular dipoles, generating structured features in the electrostatic potential of the lattice. Relativistic electronic structure reveals unique features in the bands, which may explain observed slow recombination, and could be used in high efficiency photovoltaics. The large dielectric response of the lattice leads to a strong drive for the formation of polarons, some device physics of which are discussed. These polarons offer a possible explanation for the observed slow cooling of photoexcitations in the material.

## 1. Introduction

Halide perovskites burst into the consciousness of solid-state physicists with the 2012 announcements[1, 2] of nearly 10 % power conversion efficiency solar cell devices. Mainstream silicon solar cells only recently passed 25 % efficiency, after 60 years of continuous development[3]. That halide perovskite solar cells could reach such efficiencies with relatively little research boded extremely well for the development of the technology. The active material was solution processed methylammonium lead iodide, with no vacuum or high-temperature steps in the preparation of the active material. Along with the high crustal abundance of lead and iodine, the ease of lab-scale synthesis indicated that low cost mass production would be possible.

The choice of mesoporous electrical contacts was heavily influenced by the germinal 2009[4] and 2011[5] use of the material as a dye sensitiser with a liquid electrolyte in a solar cell. The working hypothesis was that light absorbed in this material would form strongly bound excitons, charge transport would be slow, and recombination of photoexcited states fast. One therefore needs to extract the charges as fast as possible, requiring contacting on the nanometre scale.

Yet the cells could also operate when on a non-conductive alumina scaffold[2]. Planar devices[6], 100 nm thick, had an estimated 1  $\mu$ m photo-generated charge diffusion length[7].

Clearly photo-generated charges were capable of travelling a long way through the material before recombining.

The enigma from a solid-state physics point of view was and is: how can a solution-processed thin film be so efficient as a photovoltaic device? Solution-processed films are inevitably disordered and defective, yet a working photovoltaic device requires a semiconductor with sufficiently high charge-carrier mobility and low recombination velocity.

A new material with obvious technical importance presented an attractive challenge to the materials modelling community. Little was initially understood about the material. Making the experiments and building consensus in what phenomena were being observed would take time. By 2012 the materials modelling community had highly optimised codes and well understood electronic structure methods based on the highly successful density functional theory, and a wealth of computer time due to strategic investment in high performance computing. We had a unique opportunity to try and understand the material from an electronic structure perspective, and attempt to show the power of the techniques by predicting the future of what was about to be measured, rather than the less convincing argument of predicting past measurements on an already well-studied material.

## 2. Hybrid solid-state materials

Early electronic structure analysis of the material revealed unusual material properties[8]. The static dielectric constant was large ( $\epsilon = 24.1$ ) as the material is ionic and

*Email address:* jarvist.frost@imperial.ac.uk (Jarvist Moore Frost)

soft. Intriguingly, the methylammonium itself has a permanent dipole of 2.29 Debye, which appeared stable to the local polarisability[8]. This immediately implies, from knowledge that the resulting electrostatic interaction between near neighbour methylammonium is of order of the thermal energy, that a complex phase behaviour of dipole alignment will exist at room temperature. Ordering in these dipoles will result in macroscopic electric fields being generated between phases of the material, which could lead to segregation of the electron and hole charge carriers, and thus a reduction in the recombination velocity. Band alignment of the material was similar to other photovoltaic materials[9], indicating that a diversity of contact materials was possible in future device architectures. Tuning of the organic hole collecting contact seemed to be one way of modifying the open circuit voltage[10].

The simultaneous organic and inorganic nature of the material is a challenge for modelling, not least because it requires researcher knowledge of both molecular (vacuum) and solid-state (periodic) electronic structure methods. We have written a summary perspective on these challenges, suggesting guidelines for accurate calculations[11].

Solid-state electronic structure calculations usually rely on a periodicity of the lattice. This enables the calculation of the macroscopic properties of a material, by considering phase shifts within the Brillouin zone. However it relies on the perfect crystals (i.e. athermal) being representative of the material under standard (thermal) conditions.

Given the unusual hybrid nature of the material, a first question to ask is: what do the molecular dynamics look like? The first studies[12] indicated a complex array of motion on most timescales (a render of this data is available online[13]). Though the material was a crystal, it was as soft as jelly. Further studies, as summarised in our 2016 review article[14], provided an essential answer that the soft material exhibits thermally activated dynamic motion in almost every conceivable manner.

The materials are now believed to be mixed (ion and electron) conductors, and that the interaction between this conduction leads to the unusual hysteresis in device behaviour. Our early nudged elastic band calculations showed that vacancy mediated iodine motion was likely to be the major contributor[16], providing activation energies and associated predicted rates for multiple ion conduction possibilities.

One interesting aspect of the molecular dynamics of perovskite structures is that the supercell expansions used must be even. This is so that the well known perovskite tilting modes can be represented in the unit cell. (Equivalently these give rise to soft phonon modes at the relevant high symmetry point in the phonon Brillouin zone.) All tin and lead halide perovskites appear to exhibit this instability[17]. Failing to include this point (for instance a threefold rather than double expansion in one direction) leads to artificially constrained molecular dynamics.

By definition, molecular dynamics include anharmonic effects to all orders. However, the expansion of the super

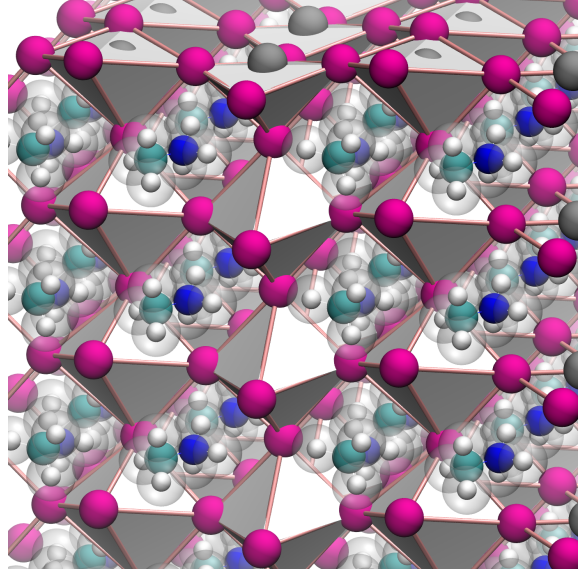


Figure 1: Rendering of a finite-temperature distorted super-cell of methylammonium lead halide perovskite. Distortions around the relaxed position are generated with a frozen-phonon approach, in this case evaluating an example of each of the first 6 branches of the phonon modes[15], at the (001) Brillouin zone location. Propagating these modes at their natural frequency (the phonon eigenvalues) allows the relative motion and harmonics between the different motion to be observed, without being obscured by the noise of an actual molecular dynamics simulation. Trajectories were generated with the JULIA-PHONONS package, visualisation by VMD and the TACHYON ray-tracer.

cell immediately quantises the phases of periodic motion that can be represented.

The main challenge of molecular dynamics is in interpreting the results, of turning the trajectories of atomic location as a function of time into something of scientific value. Qualitatively, the clear point was that the motion of the methylammonium consisted of local wobbles, followed by discrete jumps in the orientation of the methylammonium.

Early density functional theory molecular dynamics extracted a timescale of the motion[12], and by exploiting the  $O_h$  symmetry of the cubic unit cell, increased the signal to noise ratio of a measure of the orientation of the methylammonium to show that the finite temperature ensemble points at the faces (001) of the cube (along the diagonal of the octahedral pocket), as could be inferred from the relative stability of this pose from molecular statics calculations[18]. The contribution of the molecular dynamics is that it gives some idea of the occupation by the thermal ensemble, and the distribution of parameters around the minimum.

From the molecular dynamics we can directly calculate the autocorrelation time for the methylammonium motion. First analysis suggested a value of [12, 19] of 3.14 ps. This compares to a value of 14 ps (with significant error bounds) from quasi-elastic neutron scattering[19], and 3 ps from a direct infrared measurement of individual methy-

lammonium ions[20]. Intriguingly, the timescale for re-orientation of the larger formamidinium (from molecular dynamics) molecule is actually *faster* than methylammonium at 2 ps, but with a much stronger preference for (001) alignment[21]. Mixed halide materials seem to result in locked octahedral structures (due to the size mismatch), and immobilised organic cations[22].

An alternative view of the dynamics of materials is to consider harmonic expansions around the ground state structure, to calculate the normal modes of the motion and a phonon band structure. A major challenge with hybrid lead-halide materials is finding this ground state: the challenge of this procedure is in proportion to the condition number of the dynamic matrix. Containing covalent hydrogens oscillating at 90 THz and soft lead-iodide bonds with a natural frequency of 1 THz, this dynamic range makes optimisation inefficient. Much effort is therefore required to locate the structural ground state, about which the lattice dynamic perturbations can be constructed.

Interpretation of these lattice modes[15] is assisted by calculating the normal modes of the molecule in vacuum. This gives access to a classification, and infrared and Raman activity, that can be compared to the mixed modes observed in the lattice dynamics simulation. This offers a mechanistic interpretation of the observed phonon band, in terms of the well defined point-group theory and selection rules for a molecule.

We followed this work by a joint experiment (Raman) and theory study, where we attempted to pick out and identify every mode present in the dynamics, and understand how the frequencies varied across the halide series[23]. Key results here were to identify the mid-energy torsional vibration of the methylammonium C-N axis as being the molecular degree of freedom most affected by the lattice constant (halide ion), understanding the mixed transverse-linear optical modes generated by molecular coupling, and identify the ‘nodding donkey’ intermediate modes associated with the methylammonium rattling within its cage. Finally the repercussions of the large frequency range in the polar optical modes were considered.

### 3. Monte-carlo models of large scale thermal fluctuations

The methylammonium molecule possesses a permanent dipole of some 2.29 Debye. Electrostatic dipole-dipole interactions between these spins drive the formation of a columnar anti-ferroelectric phase (spins head-tail aligned), as revealed by a Metropolis Monte-Carlo lattice spin simulation[12]. This study also showed that the real-space extent of the fluctuations at room temperature was on the order of 5 unit cells.

These spin rotations do not occur in free space, but within a physical lattice, the highly anisotropic  $\text{CH}_3-\text{NH}_3$  molecules sitting within a distorted octahedral pocket. In fact, the low temperature orthorhombic phase of the material is believed to be one in which the octahedral pocket

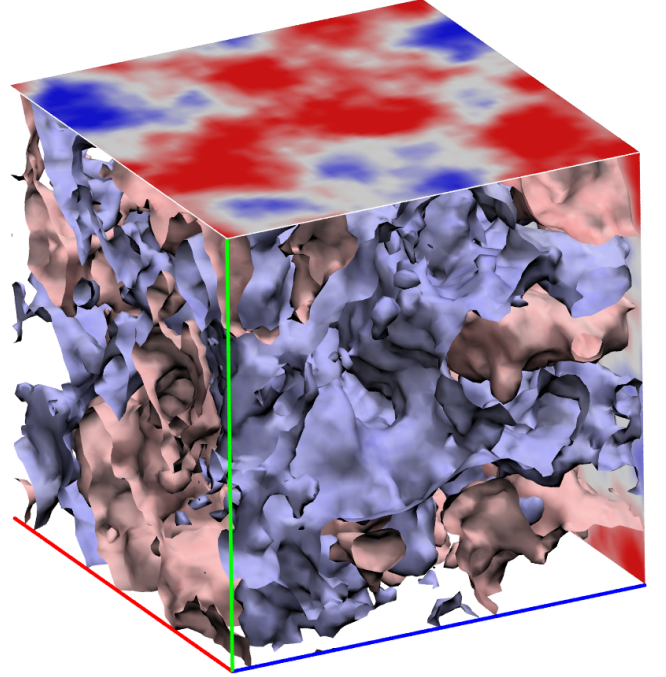


Figure 2: Simulated electrostatic potential at 300 K in a high ferroelectric driving force material, with a 50x50x50 supercell of material. The ferroelectric driving force gives rise to large regions of high (red) and low (blue) electrostatic potential. The regions are continuous (percolating). Simulated with the STARRYNIGHT codes[12, 19].

ets collapse into ordered perpendicular anti-ferroelectric terminations of the local spins. To a first approximation, the effect of this lattice confinement of the methylammonium ions is a local strain term driving alignment of co-facial methylammonium. This results in an effective dot-product energy term between nearest-neighbour spins, which can be parametrised from the constrained rotation of an individual methylammonium in a super cell as 150 meV which can be distributed between the six co-facial neighbour spins[19]. The resulting three-dimensional model is driven into a ferroelectric ground state, with larger, deeper, basins of electrostatic potential. The model can also be extended to treat defects and mixed dipole systems[24].

A challenge with such effective potential models is making strong predictions. The generated phase is the result of a careful balance of competing energy (enthalpy) terms calculated from models and approximate electronic structure methods, to which the entropic contribution is made directly by the Monte Carlo algorithm. Atomistic dynamics, even with empirical potentials[25], have difficulty in getting to the necessary simulation length and time scales to investigate such domains. Thus it is perhaps better to think of these models as predicting possibilities, with simulation temperature and the detailed values of the parameterisation to be considered variables used to reproduce and compare to the experimental reality.

A more sophisticated parameterisation of the same functional form of model was later done by Tan et al.[26]. More

understanding of the local domain structure has been provided by Li et al.[27] in terms of a ‘pair mode’ analysis of the local cluster structure.

A shortcoming of these effective potential models is that they are wholly classical. Ma and Wang took a fully randomised methylammonium orientation supercell model and provide clear indication via a linear-scaling fragment DFT method that electrostatic potential fluctuations are present in the electronic structure[28].

Empirically, no room-temperature ferroelectricity is observed from bulk electric field hysteresis measurements[29]. Yet piezo-electric force microscopy reveal an applied-field structural distortion which some authors have defined as evidence of ferroelectricity[30], columnar anti-ferroelasticity[31] whereas others believe these indicate ferroelasticity only[32]. These domains appear to disappear upon heating, as would be expected from melting the local dipole order[33].

There is currently no definitive evidence for whether there are nanometre scale potential fluctuations in the perovskite material, which would most directly affect the recombination kinetics of the photo generated charges.

#### 4. Device physics repercussions of large spin-orbit coupling

Most materials modelling is with the density functional theory. A major weakness of this electronic structure method is that band-gaps are often under predicted. In the case of lead halide perovskites, the 1 eV band-gap under prediction exhibited in a generalised-gradient approximation (GGA) functional is almost exactly balanced by a large spin-orbit coupling that reduces the band-gap by 1 eV. Forces are calculated from considering the occupied orbitals, so predicted ground state structures, lattice dynamics and molecular dynamics should be sufficiently accurate. Relying on density functional theory for details of the unoccupied orbitals, as is necessary for predictions of device behaviour, is more uncertain.

Diffraction measurements of the high temperature phases of inorganic halide perovskites solve to a cubic structure. Due to the inversion symmetry in such a structure, the Rashba effect cannot be supported and ferroelectricity cannot be present. However these coherent measurements are insensitive to disorder unless it has long range correlation.

An early high quality electronic structure calculation[34] used a full treatment of spin-orbit coupling along with a self-consistent partially-screened exchange interaction (QSGW). The unit cell was a relaxed ‘pseudo-cubic’ ferroelectric construction, where finite-temperature disorder was approximated by allowing the cell to distort and the ions to relax. This revealed an intriguing feature in the conduction band—a Rashba-Dresselhaus splitting had occurred with the spin polarised electrons being projected (in opposite, antipodal directions) away from the high-symmetry extrema.

This has obvious and severe consequences for the solar-cell device characteristics. The band-gap becomes very

slightly indirect—at low fluences the photo-excited electrons will relax into these Rashba pockets, where due to the offset in reciprocal space, there is no population of holes to recombine directly with. Effectively you have paid with enthalpy to reduce the recombination rate. A simple model based on thermal excitation back to the high-symmetry location and then direct emission (ignoring indirect transitions), predicts a 350 fold reduction in recombination due to this effect[35], with strong temperature and fluence dependent behaviour. A device level analysis by Kirchartz and Rau[36] suggests that a material with an indirect and direct gap would have an increased minority carrier lifetime, but not an increased open circuit voltage.

A second effect, as pointed out by Zheng et al.[37] is that the spin-symmetry of the electron and hole states may be incorrect for direct recombination. Combined, these two factors present in the bulk reciprocal space electronic structure may be part of the reason why recombination of minority carriers is so slow in these materials. They both arise as a result of large spin orbit coupling, interacting with a locally broken symmetry environment. Such symmetry breaking has been observed by inelastic X-ray scattering[38, 39] for the methylammonium lead halide material.

By combining molecular dynamics and frozen-phonon structures from lattice dynamics, with an electronic structure analysis of the Rashba splitting in the resulting structures[40], we found that the nature of spin-splitting in both the methylammonium and cesium lead-halide perovskites was qualitative identical at room temperature. Thermal fluctuations in all lead-halide perovskite structure are sufficient to generate these states, as the material is soft leading to distortions of the octahedra generating local polar fields intersecting with the frontier orbitals.

Measurements to confirming or contradict these suggestions from theory have been relatively slow. The total Brillouin-zone displacement is relatively small, and the materials themselves are not very stable under vacuum. The Rashba-Dresselhaus effect is driven by a local field. ARPES measurements on cleaved samples often sample surface effects; giant splitting was observed in the valence band[41], the presence of which in the bulk is not supported by any electronic structure studies.

A study of the circular galvanic effect in methylammonium lead iodide samples suggests that a spin-split indirect-gap exists at room temperature with a stabilisation energy of 110 meV[42] below the direct gap. The positive temperature dependence of the magnitude of the spin-split indicates that it may be generated by the dynamic fluctuations discussed above. The experimental value compares to predictions of 75 meV[35] for the athermal pseudo-cubic methylammonium unit cell, and 20 meV[40] for thermal ensembles of both the cesium and methylammonium.

## 5. Feynman variational polaron physics

Polarons as quasi-particles consisting of a charge carrier dressed in polar phonon excitations. The coupling of a charge carrier to a polar phonon mode, results in electron confinement. Such localisation provides a natural link between a delocalised band structure (where every electron is partially in every unit cell), and a more mechanistic device-physics picture of individual electrons discretely moving through a material. The driving force for polaron formation is the mismatch between the optical and low-frequency dielectric constants; the ionic contribution from polar phonon modes. The polarisation response of the lattice beyond the charge-carrier wavefunction envelope generates a dip in the electrostatic potential which attempts to localise the charge-carrier. The localisation renormalises the effective mass, and changes the nature of charge transport, recombination, and response to inhomogeneities in the material.

As the halide perovskites are ionic and soft, this driving force is large,  $\epsilon_{opt} = 4.5$  vs  $\epsilon_{stat} = 24.1$ [8]. Immediately this implies that polarons are likely a good representation of the charge-carriers in the material, rather than plane-waves.

The Fröhlich polaron is a simple model Hamiltonian with an effective-mass electron coupled to a polar phonon mode. The dimensionless Fröhlich parameter  $\alpha$  quantifies the dielectric electron-phonon coupling,

$$\alpha = \frac{1}{4\pi\epsilon_0} \frac{1}{2} \left( \frac{1}{\epsilon_{opt}} - \frac{1}{\epsilon_{stat}} \right) \frac{e^2}{\hbar\Omega} \left( \frac{2m_b\Omega}{\hbar} \right)^{1/2}. \quad (1)$$

Here the variables  $\epsilon_{opt}$  and  $\epsilon_{stat}$  are the optical (high frequency) and static dielectric constants (expressed in units of the permittivity of vacuum,  $\epsilon_0$ ),  $\Omega$  is the angular frequency of the polar phonon mode,  $m_b$  is the bare band effective mass. The other physical constants are  $\hbar$  the reduced Planck constant,  $e$  the electron charge.

In 2014, with a knowledge of the *QSGW* effective mass[34]  $m_e = 0.12$  (in units of the bare electron mass), the aforementioned dielectric constants, and a guess at the typical semiconductor polar phonon frequency (9 THz) this gives rise to a Fröhlich  $\alpha$  coupling parameter of 1.2[12]. The most successful solution of the Fröhlich Hamiltonian was the Feynman variational approach[43]. Here the Coulombic interaction of the charge-carrier with its lattice polarisation field, is remapped to an exactly solvable (by path integration) model of a harmonic interaction (characterised by the variable  $v$ ), decaying in time (exponential decay set by the variable  $w$ ). These  $v$  and  $w$  parameters (which are expressed in units of the angular frequency of the phonon mode  $\Omega$ ) can be freely varied to minimise the mismatch in this trial action, and the full Coloumb action, variationally approaching the true state.

For such small values of  $\alpha$  (mainly due to the light effective mass successfully resisting confinement), an asymptotic estimate of the variational solution ( $w$  fixed at 3,  $v$

linear increased with  $\alpha$ ) and a perturbative treatment of the polaron energy (and so, effective mass) is sufficient. This predicts an athermal effective mass renormalisation of +25%, and a polaron radius of 5 unit cells[12]. Considerable extra effort by Schilpf et al.[44], integrating the individual phonon contributions across the Brillouin zone, but using the same asymptotic perturbative limit of the Feynman polaron theory, improves this estimate to  $\alpha = 1.4$  and effective mass renormalisation of +28%.

The estimates of polaron extent (see equation 2.4 in [45]) come from the width of the Gaussian wavefunction which is a ground state to the harmonically bound electron and fictitious mass. This is of key importance when considering the influence of inhomogeneities in the real-space lattice. The charge-carrier state samples the lattice over the extent of its wavefunction. Fluctuations on a scale much smaller than the extent of the charge-carrier are integrated out.

## 6. Polaron mobility

To go beyond these perturbative athermal effective-mass renormalisations and directly predict the polaron features and dynamics (most importantly the temperature-dependent charge-carrier mobility), we needed to return to the original theories of Feynman et al.[46] and write computer codes to fully solve the equations of motion[47]. These codes undertake the whole computational pipeline for Feynman variation polarons for an arbitrary material, fully optimising the variational parameters by auto-differentiation of the (temperature dependent) free energies, and contour integrating the polaron response function to predict finite-temperature polaron mobility and other observables.

Reliable lattice dynamic calculations were slowed by the difficult of establishing a reliable ground-state structure about which to perturb the structure. Once this work was done, the infrared activities of individual modes can be arrived at by considering propagation of the Born effective charges along the gamma-point phonon eigenvectors[15]. The wide spectrum of polar modes with frequencies as low as 1 THz ( $\hbar\omega = 4$  meV) immediately suggests a complex temperature-activated behaviour as the polar phonon scattering modes individually start scattering as a function of charge-carrier energy and therefore temperature (see Fig. 10 in Ref. [23]). How should you marry this spectrum with the Fröhlich Hamiltonian single frequency mode?

The ultimate answer may be to extend the Feynman variational method, and explicitly consider the simultaneous action of these multiple modes numerically in the calculation of the action. Hellwarth et al.[48] provide two averaging techniques to arrive at effective frequency mode, a thermal ‘A’ technique, and an easier to apply athermal ‘B’ technique. This ‘B’ technique gives an effective optical mode frequency of 2.25 THz[49]. Combined with the effective-mass and dielectric constants as above, this gives



rise to an Fröhlich  $\alpha$  of 2.4 (for electrons in methylammonium lead iodide, see Ref. [49] for further perovskite material parameters).

Such values of  $\alpha$  are in the intermediate regime between weakly coupled (perturbative) and strongly coupled (localised, hopping) polarons. Interestingly, by virtue of their stiffer phonons and lighter effective masses, tin based halide perovskites have much smaller alpha parameters, and therefore should have less localised (more band like) charge carriers[49].

Therefore we need a temperature-dependent and non-perturbative mobility measure. The original Feynman path-integral mobility theory[46] offers exactly this, at the cost of numerically contour integrating the polaron linear-response function.

Applied to halide perovskites, this gives parameter-free temperature-dependent mobilities[49] in good agreement with (room-temperature) single-crystal measurements.

Though these predicted mobilities are numerically calculated, they are relatively featureless and monotonic, due to the athermal effective polar mode frequency. Again, a more complete result would be to extend the theories to enumerate the individual scattering modes.

One limitation of this polaron model is that the effective phonon mode is harmonic (and therefore has an infinite lifetime). In the polaron theory this leads to a resonance of energy between the electron and phonon degrees of freedom. Slower polar reorientation degrees of freedom, as would be expected from the methylammonium rearrangement, would not be harmonic. Generally the phonon modes in hybrid lead halides are predicted to be highly anharmonic[50], for which there is now some direct experimental evidence[51]. This anharmonicity broadens the spectral response, and decreases the infinite phonon lifetime to a sub-picosecond timescale. Rather than a resonant store of energy in the polaron model, these are likely to be an additional dispersive loss mechanism. The polaron theories have not yet been extended to deal with anharmonicity.

Other methods of predicting mobilities in these materials build on theories (small polaron hopping; free-electron scattering) which are not valid for the intermediate behaviour of most solid-state polar materials. They often rely on empirical parameters (such as a scattering time), which limits predictive power. Combined these problems lead to poor absolute accuracy, and incorrect predictions of temperature-dependence.

The temperature dependence of mobility ( $\mu \propto T^n$ ) can give circumstantial evidence for the nature of the scattering process controlling (limiting) mobility (see chapter 3 in Ref. [52]). Emphasising that such analysis is approximate and based on semi-classical models of mobility, acoustic deformation-potential and non-polar optical phonon mode give  $\mu \propto T^{-\frac{3}{2}}$ , whereas polar optical phonon mode scattering and acoustic phonon piezoelectric scattering give  $\mu \propto T^{-\frac{1}{2}}$ . Also note actually getting from the raw measurement to a mobility measure relies on a model of con-

ductivity, most often the classical gas Drude model. Practically speaking the values are derived by fitting a straight line to the mobility displayed on a log-log axis.

Hall-effect measurements in methylammonium lead bromide single crystals indicate an exponent of -0.5 in the low temperature phase, and -1.5 in the high temperature phase. Time-resolved terahertz conductivity measurements on methylammonium lead halide fit a  $\mu \propto T^{-\frac{3}{2}}$  relationship[53], but discounting the low temperature orthorhombic phase data and fitting to a power law in the linear (non logarithmic) metric gives a trend of -0.95[49]. This is in much closer agreement to the -0.5 from the numeric polaron theory[49]. Measurements of temperature dependent mobility on formamidinium lead iodide perovskite[54] reveal a -0.53 exponent, in almost direct agreement with the polaron model, and semi-empirical polar mode scattering.

Where does the extra scattering in the methylammonium material come from? One possibility is that is due to the formation of polar domains and resulting fluctuations in electrostatic potential[12]. Alternatively it may be the direct dielectric response of this additional dispersive polarisation response, discussed as a dielectric drag[55]. Both of these explanations invoke a unique role of the permanent 2.29 Debye dipole in methylammonium[8], but with a different mechanistic effect—either the dynamic interactions leading to a mostly-static potential landscape, or the dynamics direct interacting with the charge carriers. The two models could be distinguished by their different temperature response. It is not clear why the ‘dielectric drag’ would be greater at higher temperature, as required to increase the methylammonium temperature dependent exponent, when the dielectric response of a polar liquid *decreases* as  $\frac{1}{T}$  with temperature[56] (though the rate of response would increase with temperature). Further comparative mobility measurements of methylammonium, formamidinium and inorganic cations could inform on whether the polar-methylammonium hypothesis holds.

Overall it seems likely that a deeper understanding of transport in these materials will require a closer interaction between experiment and theory. Rather than approaching the same final phenomenological quantity of mobility from opposite directions, modelling of experimental observables would simultaneously validate the model selection, and enable stronger statistical statements to be made from both sides.

## 7. Slow cooling of photoexcited states

Another unusual behaviour noticed in the hybrid perovskite materials is slow cooling (thermalisation times exceeding nanoseconds) upon above band-gap photoexcitation[57]. This is of technical interest as such slow cooling is a prerequisite for being able to extract charges fast enough to create a hot-carrier solar cell. The measurements are challenging to interpret as there are multiple bands than can be excited in the halide perovskites, and often the bright

laser light used to get signal in the measurement takes the material into a photogenerated charge density vastly larger than that reached by a solar cell device in the dim sun, even under concentration.

The polaron model, along with the understanding that the hybrid halide perovskites have exceptionally low thermal mobility due to anharmonic coupling between the phonon modes[50], provides a simple mechanistic explanation[58]. The polaron localisation leads to a localised heating, due to the low lattice thermal conductivity, this energy takes a long time to dissipate. Thermal conductivities being ten times larger in the fully inorganic materials precludes this behaviour. The threshold ‘phonon bottleneck’ transition at higher fluence into a faster cooling regime can be understood in terms of the density at which the localised polarons start to overlap and lose their character. The material-specific localisation of the polaron gives rise to a quantised behaviour (i.e. some characteristic thermalisation time dependent only on the material, and an initial polaron temperature dependent on band-gap exceeding energy[59]).

Recently a measurements by a technique where the (thermalised) photo-excited states are reheated by a delayed infrared pulse allowed careful observation across a systematic range across the halide perovskite family[59]. Here the variations in cooling rate and density-dependence are explained by a simple mechanistic model considering the specific heat capacity (and therefore temperature reached in the localised polarons), and the characteristic timescale of optical phonon scattering (from the polaron theories) assumed proportionate to a cooling rate dominated by emission of optical phonons.

## 8. Higher lying excited states

One intriguing feature of the lead halide perovskites are the higher lying excited states, attainable with violet light (3.2 eV) in the case of the lead iodide perovskite. These states are mainly composed of Pb-6p orbitals, the same ones that make up the conduction band. But due to the spin orbital interaction, these orbitals have been pushed upwards in energy. Combined with the Rashba spin-splitting leading to incommensurate locations in reciprocal space, this suggests that an intermediate band photo ratchet[60] may be present as a bulk electronic structure effect in the material[61].

Such a mechanism would not be directly useful to make Shockley-Queisser limit exceeding photovoltaics, as the gaps in lead-halide perovskites are too high to usefully divide up the solar spectrum.

The lead-tin 50:50 alloy perovskite exhibits a much reduced 1.2 eV gap, and may offer a genuine route to higher efficiency. But the indirect band structure (therefore low oscillator strengths, therefore low photoexcited charge densities) may preclude the effect from being active[62]. Similar features may be present in other heavy-atom semi-

conductors with broken inversion symmetry, leading to a potential new class of relativistic semiconductors[63, 64].

Such higher lying states are optically accessible, and have been characterised by both ellipsometry measurements, and electronic structure[65].

Recently a fluence-independent quantum-yield of exactly 2 has been observed in CsPbI<sub>3</sub> nano-crystals upon 4.0 eV photo excitation[66]. Though this is attributed by the researchers to multiple carrier generation, the strikingly quantised quantum efficiency suggests that it may instead be sequential emission on the way down the photon ratchet. Very strong Auger recombination in these materials has been attributed to excitation to this higher energy conduction band[67], which may also be a route for carrier multiplication at high photoexcited densities.

Interesting photophysics are suggested by the relativistic band structure; interesting photophysics are being observed in the laboratory. Whether the theory explains the observations, and whether these behaviours can be made use of in a practical device, is not yet clear.

## 9. Conclusion

The five years of computational halide perovskite described in this review have benefited enormously from deep collaborations with a wide range of other research groups, both computational and experimental. Hypotheses and new ideas can be quickly and efficiently developed in pure computational studies, but the true understanding in this field has come from experiment and theory working together to understand the observed data.

We have not discussed any of the practical issues of developing a working photovoltaic technology. The two chief challenges in this area have been the stability of the material, and the fundamental economic case for switching process, to still have a standard Shockley-Queisser single band-gap technology. Much practical work now goes into tandem-cell applications, where reduced stability compared to a standard technology is a price worth to pay for the extra efficiency.

The long term benefits of the halide perovskite electronic structure studies may come from the fundamental insights offered into the observed low minority-carrier recombination rate. The two main suggestions are that this is either due to the relativistic electronic structure leading to spin-split Rashba pockets (or spin selection blocked recombination), or that the soft polar nature of the material leads to recombination pathways reduced by real-space segregation, dielectric screening and polaron effects. Further development and understanding of these processes may give guidance as to what other semiconductors can be concocted from the periodic table to give similar beneficial behaviour, without the relative instability of the halide perovskite materials.

**Acknowledgement** We thank Piers Barnes, Jenny Nelson, Mark van Schilfgaarde and Aron Walsh for many

years of stimulating discussions. Much of this work was undertaken on EPSRC Grant EP/K016288/1. J.M.F. is supported by EP/R005230/1.

## References

- [1] M. M. Lee, J. Teuscher, T. Miyasaka, T. N. Murakami, H. J. Snaith, Efficient hybrid solar cells based on meso-superstructured organometal halide perovskites, *Science* 338 (6107) (2012) 643–647. doi:10.1126/science.1228604. URL <https://doi.org/10.1126/science.1228604>
- [2] H.-S. Kim, C.-R. Lee, J.-H. Im, K.-B. Lee, T. Moehl, A. Marchioro, S.-J. Moon, R. Humphry-Baker, J.-H. Yum, J. E. Moser, M. Grätzel, N.-G. Park, Lead iodide perovskite sensitized all-solid-state submicron thin film mesoscopic solar cell with efficiency exceeding 9%, *Scientific Reports* 2 (1). doi:10.1038/srep00591. URL <https://doi.org/10.1038/srep00591>
- [3] M. A. Green, The path to 25% silicon solar cell efficiency: History of silicon cell evolution, *Progress in Photovoltaics: Research and Applications* 17 (3) (2009) 183–189. doi:10.1002/pip.892. URL <https://doi.org/10.1002/pip.892>
- [4] A. Kojima, K. Teshima, Y. Shirai, T. Miyasaka, Organometal halide perovskites as visible-light sensitizers for photovoltaic cells, *Journal of the American Chemical Society* 131 (17) (2009) 6050–6051. doi:10.1021/ja809598r. URL <https://doi.org/10.1021/ja809598r>
- [5] J.-H. Im, C.-R. Lee, J.-W. Lee, S.-W. Park, N.-G. Park, 6.5% efficient perovskite quantum-dot-sensitized solar cell, *Nanoscale* 3 (10) (2011) 4088. doi:10.1039/c1nr10867k. URL <https://doi.org/10.1039/c1nr10867k>
- [6] M. Liu, M. B. Johnston, H. J. Snaith, Efficient planar heterojunction perovskite solar cells by vapour deposition, *Nature* 501 (7467) (2013) 395–398. doi:10.1038/nature12509. URL <https://doi.org/10.1038/nature12509>
- [7] S. D. Stranks, G. E. Eperon, G. Grancini, C. Menelaou, M. J. P. Alcocer, T. Leijtens, L. M. Herz, A. Petrozza, H. J. Snaith, Electron-hole diffusion lengths exceeding 1 micrometer in an organometal trihalide perovskite absorber, *Science* 342 (6156) (2013) 341–344. doi:10.1126/science.1243982. URL <https://doi.org/10.1126/science.1243982>
- [8] J. M. Frost, K. T. Butler, F. Brivio, C. H. Hendon, M. Van Schilfgaarde, A. Walsh, Atomistic origins of high-performance in hybrid halide perovskite solar cells, *Nano letters* 14 (5) (2014) 2584–2590.
- [9] K. T. Butler, J. M. Frost, A. Walsh, Band alignment of the hybrid halide perovskites  $\text{CH}_3\text{NH}_3\text{PbCl}_3$ ,  $\text{CH}_3\text{NH}_3\text{PbBr}_3$  and  $\text{CH}_3\text{NH}_3\text{PbI}_3$ , *Materials Horizons* 2 (2) (2015) 228–231.
- [10] A. T. Murray, J. M. Frost, C. H. Hendon, C. D. Molloy, D. R. Carbery, A. Walsh, Modular design of spiro-ometad analogues as hole transport materials in solar cells, *Chemical Communications* 51 (43) (2015) 8935–8938.
- [11] L. D. Whalley, J. M. Frost, Y.-K. Jung, A. Walsh, Perspective: Theory and simulation of hybrid halide perovskites, *The Journal of chemical physics* 146 (22) (2017) 220901.
- [12] J. M. Frost, K. T. Butler, A. Walsh, Molecular ferroelectric contributions to anomalous hysteresis in hybrid perovskite solar cells, *Apl Materials* 2 (8) (2014) 081506.
- [13] J. M. Frost, Single methylammonium in mapi perovskite molecular dynamics, <https://www.youtube.com/watch?v=Rr2DDiYUoNA> (May 2014). URL <https://www.youtube.com/watch?v=Rr2DDiYUoNA>
- [14] J. M. Frost, A. Walsh, What is moving in hybrid halide perovskite solar cells?, *Accounts of chemical research* 49 (3) (2016) 528–535.
- [15] F. Brivio, J. M. Frost, J. M. Skelton, A. J. Jackson, O. J. Weber, M. T. Weller, A. R. Goni, A. M. Leguy, P. R. Barnes, A. Walsh, Lattice dynamics and vibrational spectra of the orthorhombic, tetragonal, and cubic phases of methylammonium lead iodide, *Physical Review B* 92 (14) (2015) 144308.
- [16] C. Eames, J. M. Frost, P. R. Barnes, B. C. O’reagan, A. Walsh, M. S. Islam, Ionic transport in hybrid lead iodide perovskite solar cells, *Nature communications* 6.
- [17] R. X. Yang, J. M. Skelton, E. L. Da Silva, J. M. Frost, A. Walsh, Spontaneous octahedral tilting in the cubic inorganic cesium halide perovskites  $\text{CsSnX}_3$  and  $\text{CsPbX}_3$  ( $\text{X} = \text{F}, \text{Cl}, \text{Br}, \text{I}$ ), *The journal of physical chemistry letters* 8 (19) (2017) 4720–4726.
- [18] F. Brivio, A. B. Walker, A. Walsh, Structural and electronic properties of hybrid perovskites for high-efficiency thin-film photovoltaics from first-principles, *APL Materials* 1 (4) (2013) 042111. doi:10.1063/1.4824147. URL <https://doi.org/10.1063/1.4824147>
- [19] A. M. Leguy, J. M. Frost, A. P. McMahon, V. G. Sakai, W. Kockelmann, C. Law, X. Li, F. Foglia, A. Walsh, B. C. O’reagan, et al., The dynamics of methylammonium ions in hybrid organic-inorganic perovskite solar cells, *Nature communications* 6.
- [20] A. A. Bakulin, O. Selig, H. J. Bakker, Y. L. Rezes, C. Müller, T. Glaser, R. Lovrincic, Z. Sun, Z. Chen, A. Walsh, et al., Real-time observation of organic cation reorientation in methylammonium lead iodide perovskites, *The journal of physical chemistry letters* 6 (18) (2015) 3663–3669.
- [21] M. T. Weller, O. J. Weber, J. M. Frost, A. Walsh, Cubic perovskite structure of black formamidinium lead iodide,  $\alpha\text{-[HC(NH}_2)_2\text{PbI}_3]$ , at 298 K, *The Journal of Physical Chemistry Letters* 6 (16) (2015) 3209–3212.
- [22] O. Selig, A. Sadhanala, C. Müller, R. Lovrincic, Z. Chen, Y. L. Rezes, J. M. Frost, T. L. Jansen, A. A. Bakulin, Organic cation rotation and immobilization in pure and mixed methylammonium lead-halide perovskites, *Journal of the American Chemical Society* 139 (11) (2017) 4068–4074.
- [23] A. M. A. Leguy, A. R. Goni, J. M. Frost, J. Skelton, F. Brivio, X. Rodríguez-Martínez, O. J. Weber, A. Pallipurath, M. I. Alonso, M. Campoy-Quiles, M. T. Weller, J. Nelson, A. Walsh, P. R. F. Barnes, Dynamic disorder, phonon lifetimes, and the assignment of modes to the vibrational spectra of methylammonium lead halide perovskites, *Physical Chemistry Chemical Physics* 18 (39) (2016) 27051–27066. doi:10.1039/c6cp03474h. URL <https://doi.org/10.1039/c6cp03474h>
- [24] G. Grancini, A. R. S. Kandada, J. M. Frost, A. J. Barker, M. De Bastiani, M. Gandini, S. Marras, G. Lanzani, A. Walsh, A. Petrozza, Role of microstructure in the electron–hole interaction of hybrid lead halide perovskites, *Nature photonics* 9 (10) (2015) 695–701.
- [25] A. Mattoni, A. Filippetti, M. I. Saba, P. Delugas, Methylammonium rotational dynamics in lead halide perovskite by classical molecular dynamics: The role of temperature, *The Journal of Physical Chemistry C* 119 (30) (2015) 17421–17428. doi:10.1021/acs.jpcc.5b04283. URL <https://doi.org/10.1021/acs.jpcc.5b04283>
- [26] L. Z. Tan, F. Zheng, A. M. Rappe, Intermolecular interactions in hybrid perovskites understood from a combined density functional theory and effective hamiltonian approach, *ACS Energy Letters* 2 (4) (2017) 937–942. doi:10.1021/acsenenergylett.7b00159. URL <https://doi.org/10.1021/acsenenergylett.7b00159>
- [27] J. Li, J. Järvi, P. Rinke, Multiscale model for disordered hybrid perovskites: The concept of organic cation pair modes, *Physical Review B* 98 (4). doi:10.1103/physrevb.98.045201. URL <https://doi.org/10.1103/physrevb.98.045201>
- [28] J. Ma, L.-W. Wang, Nanoscale charge localization induced by random orientations of organic molecules in hybrid perovskite  $\text{CH}_3\text{NH}_3\text{PbI}_3$ , *Nano Letters* 15 (1) (2014) 248–253. doi:10.1021/nl503494y. URL <https://doi.org/10.1021/nl503494y>
- [29] Z. Fan, J. Xiao, K. Sun, L. Chen, Y. Hu, J. Ouyang, K. P. Ong, K. Zeng, J. Wang, Ferroelectricity of  $\text{CH}_3\text{NH}_3\text{PbI}_3$  perovskite, *The Journal of Physical Chemistry Letters* 6 (7) (2015) 1155–1161. doi:10.1021/acs.jpclett.5b00389.



- URL <https://doi.org/10.1021/acs.jpcllett.5b00389>
- [30] Y. Kutes, L. Ye, Y. Zhou, S. Pang, B. D. Huey, N. P. Padture, Direct observation of ferroelectric domains in solution-processed  $\text{CH}_3\text{NH}_3\text{PbI}_3$  perovskite thin films, *The Journal of Physical Chemistry Letters* 5 (19) (2014) 3335–3339. doi:10.1021/jz501697b.  
URL <https://doi.org/10.1021/jz501697b>
- [31] H. Röhm, T. Leonhard, M. J. Hoffmann, A. Colmann, Ferroelectric domains in methylammonium lead iodide perovskite thin-films, *Energy & Environmental Science* 10 (4) (2017) 950–955. doi:10.1039/c7ee00420f.  
URL <https://doi.org/10.1039/c7ee00420f>
- [32] I. M. Hermes, S. A. Bretschneider, V. W. Bergmann, D. Li, A. Klasen, J. Mars, W. Tremel, F. Laquai, H.-J. Butt, M. Mezger, R. Berger, B. J. Rodriguez, S. A. L. Weber, Ferroelastic fingerprints in methylammonium lead iodide perovskite, *The Journal of Physical Chemistry C* 120 (10) (2016) 5724–5731. doi:10.1021/acs.jpcc.5b11469.  
URL <https://doi.org/10.1021/acs.jpcc.5b11469>
- [33] S. M. Vorpahl, R. Giridharagopal, G. E. Eperon, I. M. Hermes, S. A. L. Weber, D. S. Ginger, Orientation of ferroelectric domains and disappearance upon heating methylammonium lead triiodide perovskite from tetragonal to cubic phase, *ACS Applied Energy Materials* 1 (4) (2018) 1534–1539. doi:10.1021/acs.aem.7b00330.  
URL <https://doi.org/10.1021/acs.aem.7b00330>
- [34] F. Brivio, K. T. Butler, A. Walsh, M. van Schilfgaarde, Relativistic quasiparticle self-consistent electronic structure of hybrid halide perovskite photovoltaic absorbers, *Physical Review B* 89 (15). doi:10.1103/physrevb.89.155204.  
URL <https://doi.org/10.1103/physrevb.89.155204>
- [35] P. Azarhoosh, S. McKechnie, J. M. Frost, A. Walsh, M. van Schilfgaarde, Research update: Relativistic origin of slow electron-hole recombination in hybrid halide perovskite solar cells, *APL Materials* 4 (9) (2016) 091501. doi:10.1063/1.4955028.  
URL <https://doi.org/10.1063/1.4955028>
- [36] T. Kirchartz, U. Rau, Decreasing radiative recombination coefficients via an indirect band gap in lead halide perovskites, *The Journal of Physical Chemistry Letters* 8 (6) (2017) 1265–1271. doi:10.1021/acs.jpcllett.7b00236.  
URL <https://doi.org/10.1021/acs.jpcllett.7b00236>
- [37] F. Zheng, L. Z. Tan, S. Liu, A. M. Rappe, Rashba spin-orbit coupling enhanced carrier lifetime in  $\text{CH}_3\text{NH}_3\text{PbI}_3$ , *Nano Letters* 15 (12) (2015) 7794–7800. doi:10.1021/acs.nanolett.5b01854.  
URL <https://doi.org/10.1021/acs.nanolett.5b01854>
- [38] A. N. Beecher, O. E. Semonin, J. M. Skelton, J. M. Frost, M. W. Terban, H. Zhai, A. Alatas, J. S. Owen, A. Walsh, S. J. Billinge, Direct observation of dynamic symmetry breaking above room temperature in methylammonium lead iodide perovskite, *ACS Energy Letters* 1 (4) (2016) 880–887.
- [39] R. Comin, M. K. Crawford, A. H. Said, N. Herron, W. E. Guise, X. Wang, P. Amela S. Whitfield, A. Jain, X. Gong, A. J. H. McGaughey, E. H. Sargent, Lattice dynamics and the nature of structural transitions in organolead halide perovskites, *Physical Review B* 94 (9). doi:10.1103/physrevb.94.094301.  
URL <https://doi.org/10.1103/physrevb.94.094301>
- [40] S. McKechnie, J. M. Frost, D. Pashov, P. Azarhoosh, A. Walsh, M. van Schilfgaarde, Dynamic symmetry breaking and spin splitting in metal halide perovskites, *Physical Review B* 98 (8) (2018) 085108.
- [41] D. Niesner, M. Wilhelm, I. Levchuk, A. Osvet, S. Shrestha, M. Batentschuk, C. Brabec, T. Fauster, Giant Rashba splitting in  $\text{CH}_3\text{NH}_3\text{PbBr}_3$  organic-inorganic perovskite, *Physical Review Letters* 117 (12). doi:10.1103/physrevlett.117.126401.  
URL <https://doi.org/10.1103/physrevlett.117.126401>
- [42] D. Niesner, M. Hauck, S. Shrestha, I. Levchuk, G. J. Matt, A. Osvet, M. Batentschuk, C. Brabec, H. B. Weber, T. Fauster, Structural fluctuations cause spin-split states in tetragonal  $(\text{CH}_3\text{NH}_3)\text{PbI}_3$  as evidenced by the circular photogalvanic effect, *Proceedings of the National Academy of Sciences* 115 (38) (2018) 9509–9514. doi:10.1073/pnas.1805422115.  
URL <https://doi.org/10.1073/pnas.1805422115>
- [43] R. P. Feynman, Slow electrons in a polar crystal, *Physical Review* 97 (3) (1955) 660–665. doi:10.1103/physrev.97.660.  
URL <https://doi.org/10.1103/physrev.97.660>
- [44] M. Schlipf, S. Poncé, F. Giustino, Carrier lifetimes and polaronic mass enhancement in the hybrid halide perovskite  $\text{CH}_3\text{NH}_3\text{PbI}_3$  from multiphonon Fröhlich coupling, *Physical Review Letters* 121 (8). doi:10.1103/physrevlett.121.086402.  
URL <https://doi.org/10.1103/physrevlett.121.086402>
- [45] T. D. Schultz, Slow electrons in polar crystals: Self-energy, mass, and mobility, *Physical Review* 116 (3) (1959) 526–543. doi:10.1103/physrev.116.526.  
URL <https://doi.org/10.1103/physrev.116.526>
- [46] R. P. Feynman, R. W. Hellwarth, C. K. Iddings, P. M. Platzman, Mobility of slow electrons in a polar crystal, *Physical Review* 127 (4) (1962) 1004–1017. doi:10.1103/physrev.127.1004.  
URL <https://doi.org/10.1103/physrev.127.1004>
- [47] J. M. Frost, PolaronMobility.jl: Implementation of the Feynman variational polaron model, *Journal of Open Source Software* 3 (28) (2018) 566. doi:10.21105/joss.00566.  
URL <https://doi.org/10.21105/joss.00566>
- [48] R. W. Hellwarth, I. Biaggio, Mobility of an electron in a multimode polar lattice, *Physical Review B* 60 (1) (1999) 299–307. doi:10.1103/physrevb.60.299.  
URL <https://doi.org/10.1103/physrevb.60.299>
- [49] J. M. Frost, Calculating polaron mobility in halide perovskites, *Physical Review B* 96 (19) (2017) 195202.
- [50] L. D. Whalley, J. M. Skelton, J. M. Frost, A. Walsh, Phonon anharmonicity, lifetimes, and thermal transport in  $\text{CH}_3\text{NH}_3\text{PbI}_3$  from many-body perturbation theory, *Physical Review B* 94 (22) (2016) 220301.
- [51] A. Gold-Parker, P. M. Gehring, J. M. Skelton, I. C. Smith, D. Marshall, J. M. Frost, H. I. Karunadasa, A. Walsh, M. F. Toney, Acoustic phonon lifetimes limit thermal transport in methylammonium lead iodide, *arXiv preprint arXiv:1807.06679*.
- [52] B. K. Ridley, *Quantum Processes in Semiconductors*, Oxford University Press, 2013.
- [53] R. L. Milot, G. E. Eperon, H. J. Snaith, M. B. Johnston, L. M. Herz, Temperature-dependent charge-carrier dynamics in  $\text{CH}_3\text{NH}_3\text{PbI}_3$  perovskite thin films, *Advanced Functional Materials* 25 (39) (2015) 6218–6227. doi:10.1002/adfm.201502340.  
URL <https://doi.org/10.1002/adfm.201502340>
- [54] C. L. Davies, J. Borchert, C. Q. Xia, R. L. Milot, H. Kraus, M. B. Johnston, L. M. Herz, Impact of the organic cation on the optoelectronic properties of formamidinium lead triiodide, *The Journal of Physical Chemistry Letters* 9 (16) (2018) 4502–4511. doi:10.1021/acs.jpcllett.8b01628.  
URL <https://doi.org/10.1021/acs.jpcllett.8b01628>
- [55] M. Bonn, K. Miyata, E. Hendry, X.-Y. Zhu, Role of dielectric drag in polaron mobility in lead halide perovskites, *ACS Energy Letters* 2 (11) (2017) 2555–2562. doi:10.1021/acsenenergylett.7b00717.  
URL <https://doi.org/10.1021/acsenenergylett.7b00717>
- [56] J. G. Kirkwood, The dielectric polarization of polar liquids, *The Journal of Chemical Physics* 7 (10) (1939) 911–919. doi:10.1063/1.1750343.  
URL <https://doi.org/10.1063/1.1750343>
- [57] M. B. Price, J. Butkus, T. C. Jellicoe, A. Sadhanala, A. Briane, J. E. Halpert, K. Broch, J. M. Hodgkiss, R. H. Friend, F. Deschler, Hot-carrier cooling and photoinduced refractive index changes in organic-inorganic lead halide perovskites, *Nature Communications* 6 (1). doi:10.1038/ncomms9420.  
URL <https://doi.org/10.1038/ncomms9420>
- [58] J. M. Frost, L. D. Whalley, A. Walsh, Slow cooling of hot polarons in halide perovskite solar cells, *ACS energy letters* 2 (12) (2017) 2647–2652.
- [59] T. R. Hopper, A. Gorodetsky, J. M. Frost, C. Müller, R. Lovrinčić, A. A. Bakulin, Ultrafast intraband spectroscopy of hot-

- carrier cooling in lead-halide perovskites, *ACS Energy Letters* doi:10.1021/acsenenergylett.8b01227.  
URL <https://doi.org/10.1021/acsenenergylett.8b01227>
- [60] M. Yoshida, N. J. Ekins-Daukes, D. J. Farrell, C. C. Phillips, Photon ratchet intermediate band solar cells, *Appl. Phys. Lett.* 100 (26) (2012) 263902. doi:10.1063/1.4731277.  
URL <http://dx.doi.org/10.1063/1.4731277>
- [61] J. M. Frost, P. Azarhoosh, S. McKechnie, M. van Schilfgaarde, A. Walsh, A photon ratchet route to high-efficiency hybrid halide perovskite intermediate band solar cells, *arXiv preprint arXiv:1611.09786*.
- [62] A. Goyal, S. McKechnie, D. Pashov, W. Tumas, M. van Schilfgaarde, V. Stevanović, Origin of pronounced nonlinear band gap behavior in lead-tin hybrid perovskite alloys, *Chemistry of Materials* 30 (11) (2018) 3920–3928. doi:10.1021/acs.chemmater.8b01695.  
URL <https://doi.org/10.1021/acs.chemmater.8b01695>
- [63] K. T. Butler, S. McKechnie, P. Azarhoosh, M. van Schilfgaarde, D. O. Scanlon, A. Walsh, Quasi-particle electronic band structure and alignment of the v-VI-VII semiconductors SbSI, SbSBr, and SbSeI for solar cells, *Applied Physics Letters* 108 (11) (2016) 112103. doi:10.1063/1.4943973.  
URL <https://doi.org/10.1063/1.4943973>
- [64] K. T. Butler, J. M. Frost, A. Walsh, Ferroelectric materials for solar energy conversion: photoferroics revisited, *Energy & Environmental Science* 8 (3) (2015) 838–848.
- [65] A. M. A. Leguy, P. Azarhoosh, M. I. Alonso, M. Campoy-Quiles, O. J. Weber, J. Yao, D. Bryant, M. T. Weller, J. Nelson, A. Walsh, M. van Schilfgaarde, P. R. F. Barnes, Experimental and theoretical optical properties of methylammonium lead halide perovskites, *Nanoscale* 8 (12) (2016) 6317–6327. doi:10.1039/c5nr05435d.  
URL <https://doi.org/10.1039/c5nr05435d>
- [66] C. de Weerd, L. Gomez, A. Capretti, D. M. Lebrun, E. Matsumura, J. Lin, M. Ashida, F. C. M. Spoor, L. D. A. Siebbeles, A. J. Houtepen, K. Suenaga, Y. Fujiwara, T. Gregorkiewicz, Efficient carrier multiplication in CsPbI<sub>3</sub> perovskite nanocrystals, *Nature Communications* 9 (1). doi:10.1038/s41467-018-06721-0.  
URL <https://doi.org/10.1038/s41467-018-06721-0>
- [67] J.-X. Shen, X. Zhang, S. Das, E. Kioupakis, C. G. V. de Walle, Unexpectedly strong auger recombination in halide perovskites, *Advanced Energy Materials* 8 (30) (2018) 1801027. doi:10.1002/aenm.201801027.  
URL <https://doi.org/10.1002/aenm.201801027>